Iraqi Journal of Oil & Gas Research
Journal homepage: https://ijogr.uotechnology.edu.iq

Spatial Distribution and Petrophysical Characterization of Reservoir Rocks in the AB Unit

[1]Esra Q. Saleh[*], [1]Alaa M. Atiaa and [1]Amna M. Handhal
[1] Geology Department, University of Basrah-Iraq, Basra,

Article information

Article history:

Received: August, 25, 2023
Accepted: October, 06, 2023
Available online: October, 08, 2023

Keywords:
Petrophysics,
AB unit,
Well logs,
Spatial distribution,
Ordinary Kriging

Corresponding Author:
Esraa. Q. Saleh ealqanas@gmail.com

Abstract

Hydrocarbon exploration and production heavily rely on understanding the petrophysical properties and spatial distribution of reservoir rocks. This study delves into an in-depth analysis of the AB unit's petrophysical attributes, with a specific focus on its spatial distribution and lithological identification. The research encompasses a comprehensive investigation of essential petrophysical properties, including porosity, permeability, and fluid saturation, shedding light on their significance in effective reservoir evaluation and optimized hydrocarbon extraction. The intricate nature of the AB unit's petrophysical characteristics is unraveled by harnessing the power of well logs, which encompass gamma-ray, resistivity, density, and neutron logs. This comprehensive characterization is further corroborated and validated through rigorous statistical analysis. Moreover, an exploration into the spatial distribution of these petrophysical attributes is undertaken, employing the sophisticated geostatistical technique known as Ordinary Kriging. The results of this analysis reveal distinct patterns of porosity, permeability, and lithology, providing valuable insights for reservoir management and decision-making. The findings of this study contribute significantly to a holistic understanding of the AB unit's reservoir potential, thereby guiding prudent exploration, production, and development strategies. Results showed that most reservoirs contain hydrocarbons. Porosity throughout the reservoirs ranged from 0.06 to 0.20; permeability ranged from 1.58 to 624.34md; and average hydrocarbon saturation was 68.14%. These findings point to a reservoir system with a significant hydrocarbon potential and acceptable performance for hydrocarbon production.

DOI: http://doi.org/10.55699/ijogr.2023.0302.1053, Oil and Gas Engineering Department, University of Technology-Iraq

1. Introduction

The exploration and exploitation of hydrocarbon reservoirs require a deep understanding of petrophysical characteristics and the spatial distribution of reservoir rocks. Petrophysics, as a discipline, focuses on the study of porous media, encompassing reservoir rocks and the fluids they contain, along with their fundamental chemical and physical attributes. Key aspects under scrutiny include the capacity to store and transport fluids (porosity, permeability, and fractional flow), the ability to discern various fluids, the distribution of fluid phases within the pore space (saturation), interactions between rock and fluid surface forces (capillary pressure), the measurement of pressure and stress conditions, and the electrical conductivity of fluid-saturated rocks, among others **[1]**. Petrophysical properties play a pivotal role in determining the storage and productivity potential of hydrocarbon reservoirs. Thorough analysis of rock features and fluid-filled pores offers valuable insights into reservoir behavior and production capabilities. Essential petrophysical parameters encompass porosity, permeability, water saturation, lithology, and shale volume, all of which form the bedrock of reservoir analysis. Porosity, indicative of pore volume within a rock, directly influences its capacity to hold fluids like water, gas, or oil. Permeability dictates pore connectivity and fluid mobility within the reservoir. Water saturation estimation unveils the proportion of pore space occupied by water, a critical factor for assessing hydrocarbon reserves and optimizing extraction methods. Lithology provides insights into rock texture and composition, while shale volume exerts a substantial impact on reservoir porosity and permeability. Proficiency in understanding these petrophysical properties is paramount for effective reservoir assessment and hydrocarbon extraction strategies.

The AB unit, nestled within a hydrocarbon-rich formation, serves as the focal point of this study. Given the paramount importance of petrophysical properties in reservoir management, this research endeavors to unravel the intricate attributes characterizing the AB unit. This exploration aims to enhance the efficiency and effectiveness of hydrocarbon exploration, extraction, and field development. Petrophysics plays a pivotal role in any oilfield, encompassing an in-depth evaluation of reservoir rock and fluid characteristics that significantly influence oil recovery and production volumes. These characteristics encompass key parameters such as porosity, permeability, fluid saturation, and shale volume. Robust assessments of these components facilitate predictions regarding the complex behavior of reservoir conditions and the estimation of a reservoir's hydrocarbon-holding capacity and performance [2]. The quantity of initially present oil and gas reserves is primarily dictated by rock porosity and fluid saturations, while permeability defines the ease of fluid flow through the rock's pore spaces. These factors are pivotal in the domain of reservoir engineering [3].

The Zubair Formation constitutes a substantial oil-producing reservoir within the South Rumaila oil field in Iraq. The AB unit, a component of the Zubair Formation, is distinguished by its high permeability and porosity, rendering it an attractive target for oil production [4]. Understanding the petrophysical properties of this unit holds significant importance in the context of managing oil production and water injection programs. Consequently, this study leveraged conventional well logs, including the Lateral Log Deep (LLD) resistivity log, the density log (PHID), the gamma-ray log, and the neutron log (PHIN), to ascertain the petrophysical characteristics of the AB unit and to differentiate between hydrocarbon-bearing and non-hydrocarbon-bearing zones. The primary petrophysical properties under examination in this study encompass porosity, permeability, water and hydrocarbon saturations, and the volume of shale. This comprehensive analysis seeks to provide valuable insights into the reservoir's potential and performance, thereby guiding prudent reservoir management practices and hydrocarbon extraction strategies. The primary objective of this investigation is to gain a comprehensive understanding of the fundamental petrophysical attributes, specifically porosity, permeability, and volume of shale within the AB reservoir unit. Additionally, this study seeks to delineate the spatial distribution of these critical petrophysical parameters.

2. Geological setting:

The Rumaila oilfield is a huge oilfield in southern Iraq that lies 32 km from the Kuwaiti boundary (Figure 1). The oilfield covers an area of about 1600 km2. The top portion of the Zubair Formation in the Rumila oil field is the study's primary focus. The Rumaila is made up of one main fold that spans from the southern Kuwaiti border to the northern part Al-Hammar marsh and is composed of three domes [5]. The names of these three domes are Southern Rumaila, Northern Rumaila, and West Qurna, respectively. They make up an oil structure that is over 100 kilometers long and 15 kilometers broad when taken as a whole [6]. The Rumaila field is home to a variety of sedimentary rocks, ranging in age from Late Jurassic to Recent [5]. The most significant hydrocarbon system in this stratigraphic column is the Early Cretaceous–Miocene petroleum system. This

system is made up of source rocks, sealing rocks, and reservoir rocks. Within this system, the Sulaiy and Yamama formations serve as source rocks, while the Tanuma, Shranish, and Rus formations act as sealing rocks. The Yamama, Zubair, Nahr Umr, and Mishrif formations are reservoir rocks [7]. The Zubair Formation is the most important reservoir rock in the Rumaila field. It is composed of fluvial-deltaic marine sandstones that were deposited during the Hauterivian-early Aptian stages of the Early Cretaceous period [8]. The average thickness of the formation is 425 meters, and it is overlain by the Shuaiba Formation and underlain by the Ratawi Formation. The upper sandstone member of the Zubair Formation is the focus of the present study. It is located at an average depth of approximately 3150 meters below mean sea level and consists of sandstones with some interbedded shales. The total thickness of the reservoir is about 145 meters, and it contains three reservoir units (Figure 2): AB, DJ, and LN. The AB unit is the smallest and most widespread reservoir unit, and it ranges in thickness from 2.8 to 14 meters. The DJ unit is the thickest reservoir unit, and it ranges in thickness from 46 to 66 meters. The LN unit is the third reservoir unit, and it ranges in thickness from 30 to 53 meters. The reservoir units are separated into two isolating units: C and K. Unit C is located between the AB and DJ units, and it is composed of shale and siltstone. Unit K is located between the DJ and LN units, and it is composed of siltstone and shale.

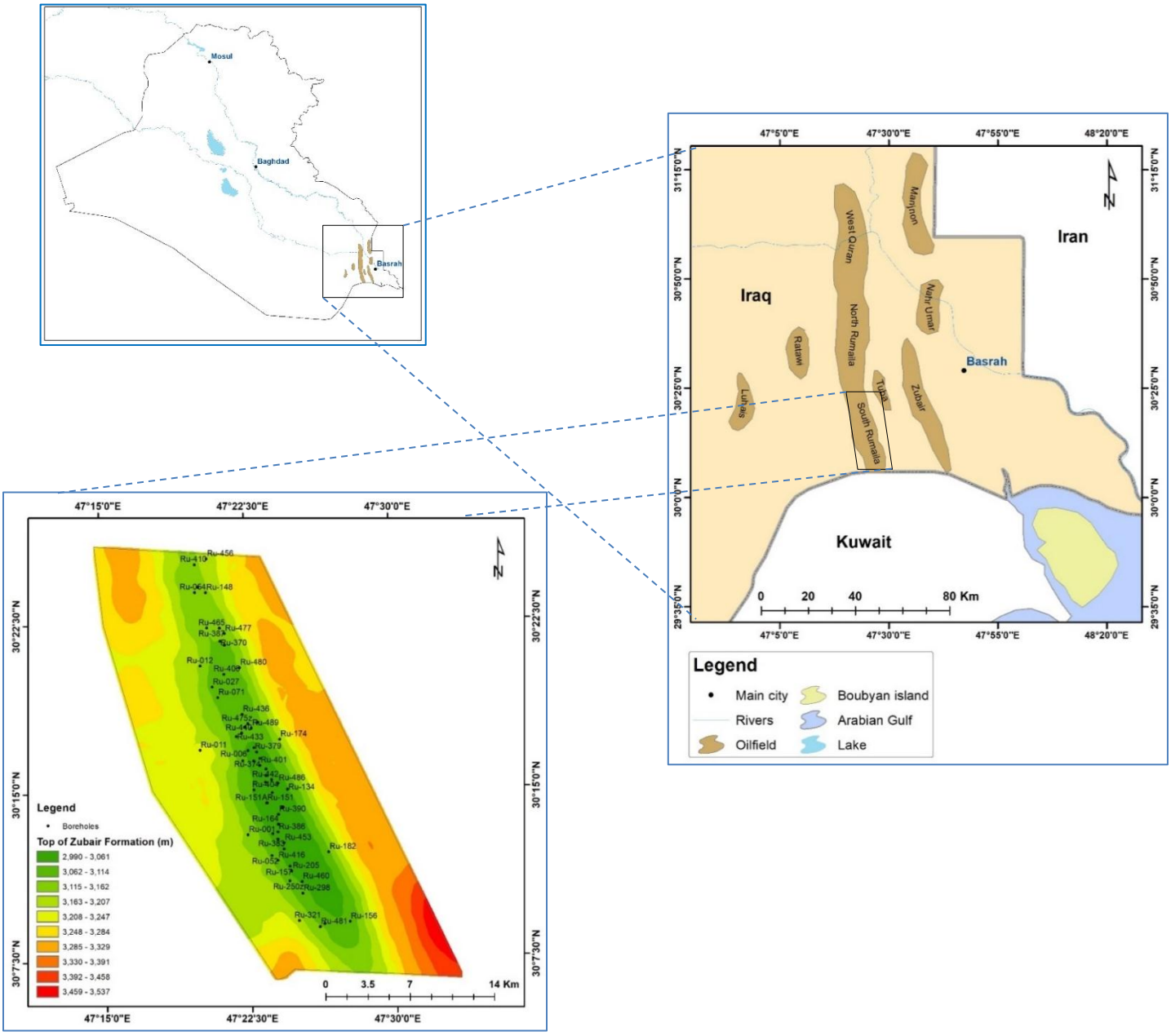

Figure 1: Location of the study area

The AB unit in the southern Rumaila oil field in southern Iraq is an important component of the Zubair Formation, a Late Cretaceous sandstone-dominant reservoir that is known for its high permeability and porosity. The AB unit has been estimated to hold over 1 billion barrels of recoverable oil. This unit is considered a key contributor to the overall production from the southern Rumaila oil field, which is one of the largest in Iraq. The field is being developed by international oil companies, and their efforts to maximize production from the AB unit and other parts of the field have been well-documented in various industry reports. For example, a report by the Iraq Oil Report (2021) states that the AB unit is a focus of production optimization efforts in the southern Rumaila oil field. These references highlight the significance of the AB unit in the southern Rumaila oil field and its importance as a source of oil for Iraq.

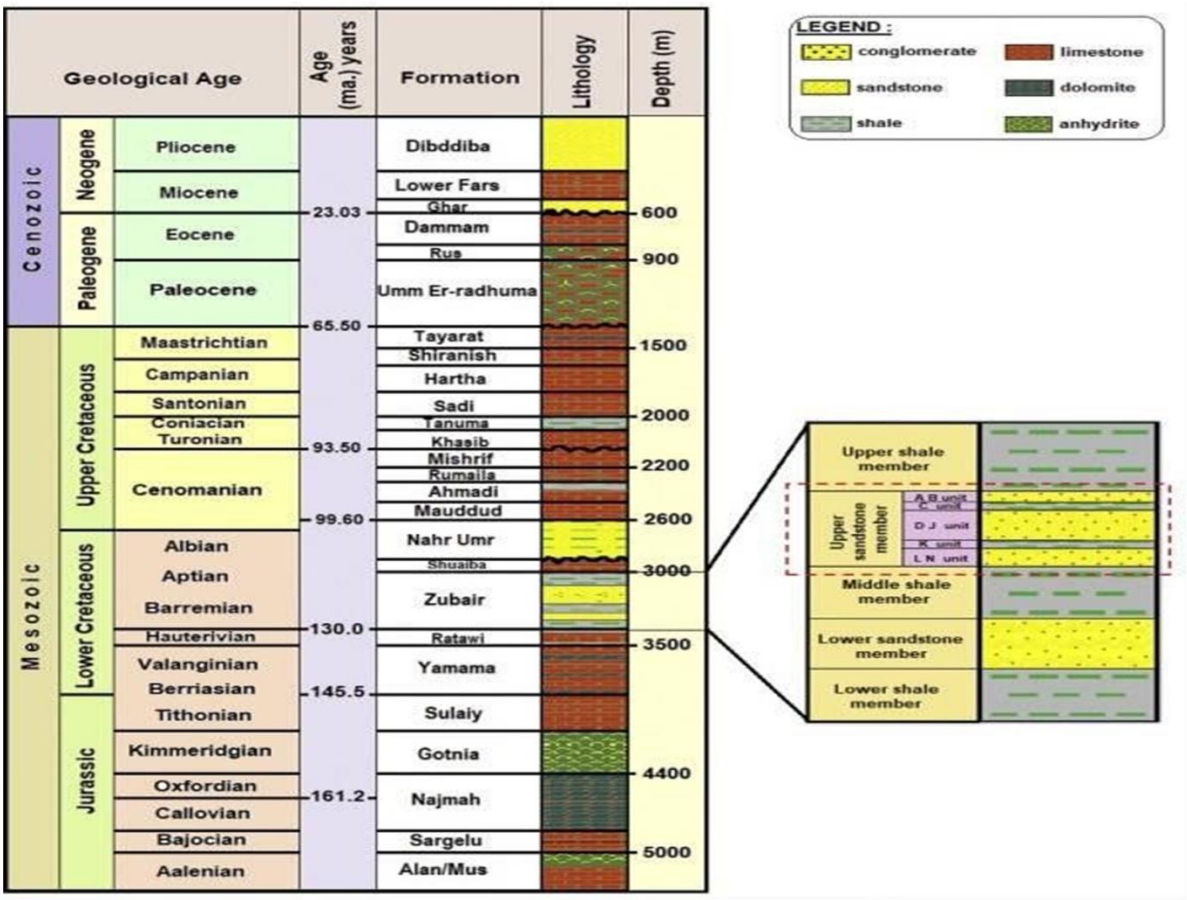

Figure 2: Stratigraphic column of Rumaila oilfield (After Handhal et al.,2018)

3. Materials and methods

In this research, work was conducted in 45 wells distributed in a way that covers the study area, and the thickness of the AB unit is different in these wells, and the thickness of the AB unit ranges from (3.5-13.87) with an average of 9.37. The density log, gamma ray log, neutron log, and resistivity log were mainly used in

this study to calculate the petrophysical properties of these wells.

3.1 Well Logging and Logs Used: Well logging emerges as an indispensable tool in the arsenal of reservoir characterization techniques. A wealth of information concerning the subsurface formations is accessed through the deployment of well logs. The utilization of various logs, including gamma-ray, resistivity, density, and neutron logs, enables us to elucidate the petrophysical characteristics of the AB unit. These logs, each with its distinct measurement principle, contribute to the comprehensive analysis of lithology, fluid identification, and reservoir properties.

3.1.1 Gamma-ray log (GR): The gamma-ray log serves as a reliable indicator of lithological variations within subsurface formations. By detecting natural radioactivity arising from elements such as uranium, potassium, and thorium, this log aids in differentiating reservoir rocks from non-reservoir rocks, a critical aspect of lithological identification.

3.1.2 Resistivity log: The resistivity log, a workhorse of well logging techniques, provides valuable insights into the electrical resistivity of subsurface formations. This property, indicative of the rock's composition, fluid content, and connectivity, is pivotal in deciphering reservoir behavior, characterizing fluids, and estimating rock properties such as porosity and permeability.

3.1.3 Density log: The density log assumes significance in lithology identification and porosity estimation. By measuring the bulk density of subsurface formations, this log aids in distinguishing different lithologies, particularly those characterized by varying densities. Moreover, it offers insights into porosity variations, a crucial parameter in reservoir evaluation.

3.1.4 Neutron log: The neutron log is a dedicated porosity log that relies on the interaction between emitted neutrons and hydrogen atoms within the formation. This interaction provides insights into porosity estimation and fluid identification. While its utility is evident in water and oil-filled formations, gas-filled formations necessitate corrections due to the gas effect.

3.2 Lithological Identification: Lithological identification stands as a cornerstone in reservoir characterization. The integration of gamma-ray, neutron, and density logs empowers geoscientists to demarcate lithological boundaries within the AB unit. A comprehensive understanding of the reservoir's composition and its implications for hydrocarbon exploration is obtained by leveraging the distinct responses of these logs to varying lithologies.

3.3 Petrophysical Measurements:

3.3.1 Volume of shale (Vsh): Shale, a ubiquitous presence in subsurface formations, exerts a significant influence on petrophysical properties. The estimation of shale volume (Vsh) assumes paramount importance in accurate porosity and permeability determination. The reservoir's petrophysical properties, such as its total and effective porosity, permeability, and water saturation, are significantly impacted by the presence of shale in the formation. Its existence in oil reservoirs does not provide a reliable evaluation of the reservoir or a reliable estimation of the reserves of oil and gas [9]. Therefore, the information for the shale volume (Vsh) must be determined. According to [10] and [11], the GR log is the most accurate method for calculating the shale volume (Vsh), computed as follows:

$$V_{sh} = 0.33 \times \left(2^{(2 \times I_{GR})} - 1\right) \quad (1)$$

Where V_{sh} = Volume of shale, I_{GR} = gamma ray index.

The shale volume V_{sh} is initially calculated from the gamma-ray index [11] using the following relationship.

$$I_{GR} = \frac{GR_{log} - GR_{min}}{GR_{max} - GR_{min}} \quad (2)$$

The values are defined as follows:

I_{GR}= gamma ray index, GR_{log}= gamma ray reading of formation, API

GR_{min}= minimum gamma ray (clean sand) API, GR_{max}= maximum gamma ray (shale), API

3.3.2 Porosity (ϕ): Porosity, the ratio of void volume to total rock volume, stands as a bedrock parameter in reservoir evaluation. The estimation of porosity is multifaceted, involving techniques such as density porosity and neutron density porosity.

3.3.2.1 Density porosity: Measurements obtained from well logs provide an indirect means of determining

porosity values in reservoir rocks. By combining two or more logs, it is possible to obtain accurate estimates of porosity. Among the various well logs, the density log is considered one of the most reliable and widely used for porosity determination. The density log calculates porosity using the following equation [12]:

$$\phi_D = \frac{(\rho_{ma} - \rho_b)}{(\rho_{ma} - \rho_f)} \quad (3)$$

Where: $\phi_D$is density porosity, $\rho_{ma}$is matrix density, ρ_b is bulk density (read from density log), and ρ_f is fluid density.
The Dresser Atlas equation [13] must be utilized to get around the shale effect in order to measure porosity in a deposit with more than 10% shale volume:

$$\phi_{Dcorr} = \left[\frac{\rho_{ma} - \rho_b}{\rho_{ma} - \rho_f}\right] - V_{sh}\left[\frac{\rho_{ma} - \rho_{sh}}{\rho_{ma} - \rho_f}\right] \quad (4)$$

Where: ϕ_{Dcorr} is correction of density porosity, V_{sh} is shale volume, and ρ_{sh} is density of shale.

3.3.2.2. Neutron density: The porosity can be calculated directly from the neutron log based on the interaction between fast neutrons emitted by the log and the hydrogen atoms present in the fluids such as water and hydrocarbon. When the reservoir contains more than 10% of the shale, the neutron porosity values must be corrected using the following equation [14]:

$$\phi_{N\,corr} = \phi_{N\,log} - (\phi_{N\,sh} * V_{sh}) \quad (5)$$

Where: $\phi_{N\,corr}$ is correct neutron porosity, $\phi_{N\,log}$ is neutron porosity from log and $\phi_{N\,sh}$ neutron porosity for shale.
By the combination of neutron–density logs, the total porosity within reservoirs interval was determined. The equation to compute the total porosity from neutron and density logs that may be expressed as [12]:

$$\phi_t = \frac{(\phi_D + \phi_N)}{2} \quad (6)$$

While the effective porosity can be calculated from the following equation [12]:

$$\phi_e = \frac{\phi_{D\,corr} + \phi_{N\,cor}}{2} * (1 - V_{sh}) \quad (7)$$

Where: ϕ_t is total porosity and ϕ_e is effective porosity.

3.3.3 Permeability: Permeability, a key determinant of fluid flow within reservoir rocks, influences production rates and recovery strategies. Through core analysis using Constant-Rate-of-Flow (CRF) and Constant-Pressure-Drop (CPD) tests, permeability values were extracted. These values, pivotal in reservoir management decisions, contribute to a comprehensive understanding of the AB unit's hydrocarbon potential [15].
Permeability is assessed through various methods, including a traditional approach that establishes correlations between permeability and core-derived porosity data. This enables estimation of permeability in unexplored areas using logarithm-derived porosity as in the equation below [16]

$$K = a \times e^{b}\phi \quad (8)$$

Additionally, Wylie and Rose introduced a method linking permeability to porosity (ϕ) and irreducible water

saturation (Swi), offering a comprehensive perspective on permeability determination [17]

$$K = a\left(\frac{\phi^b}{Swi^c}\right) \quad (9)$$

Kozeny's 1927 formula remains pivotal, providing valuable insights into permeability estimation [18]

$$K = a\left(\frac{\phi}{s}\right) \quad (10)$$

These approaches offer diverse tools for assessing and characterizing reservoir permeability, vital for efficient hydrocarbon exploration and production.

3.3.4 Fluid Saturation: Fluid saturation, a linchpin in reservoir assessment, entails the estimation of water and hydrocarbon content within formations.

To calculate fluid saturation, it is necessary to discriminate between the various fluid contents (water and oil) that fill pore spaces in both the flushed and invaded zone. The most crucial stage in the interpretation of logs is water saturation. According to [19], For estimating hydrocarbon saturation (S_h), apply the equation below:

$$S_h = 1 - S_w \quad (11)$$

In the invaded zone at the depths where shale concentration is below 10%, the water saturation was calculated using the equation shown below [20]

$$S_w = \left[\frac{F*R_w}{R_t}\right]^{1/\mathrm{n}} \quad (12)$$

Where: S_w = water saturation of the uninvaded zone, fraction, F = formation factor of the reservoir, R_w = resistivity of formation water, Ω.m, R_t= true formation resistivity, Ω.m, n = saturation exponent.

It is important to understand how to calculate the variables in the Archie equations before using them and determine the formation factor (F)

According to Archie's 1942 explanation, a constant known as the formation factor (F) links the resistivity of a formation that is 100% saturated with formation water to the resistivity of water formation (R_w)

$$R_\circ = F * R_w \quad (13)$$

Additionally, Archie provided the following equation to demonstrate how the formation factor (F) and formation porosity are related:

$$F = \frac{\varepsilon}{\emptyset^m} \quad (14)$$

Where: m = cementation factor, ε = tortuosity factor

Additionally, the determination of moveable hydrocarbon index (MHI) aids in assessing hydrocarbon movement during invasion, contributing to efficient production strategies.

3.4. Statistical Analysis of Petrophysical Properties: Intricately woven into the fabric of reservoir characterization is statistical analysis, shedding light on the variability and distribution of petrophysical properties. The exploration of probability distributions, skewness, kurtosis, and coefficient of variation yields crucial insights into the nature of the data. These statistical measures provide a deeper understanding of porosity, permeability, water saturation, and shale volume, enabling informed decision-making.

3.5. Spatial Distribution Analysis: The significance of spatial distribution analysis is underscored by its pivotal role in reservoir management and decision-making. Ordinary Kriging, a geostatistical technique, is a powerful tool for generating spatial maps of petrophysical properties. It creates property maps by interpolating data points using weighted averages, depicting variations within the reservoir. The Kriging variance measures uncertainty, enhancing map reliability and aiding in uncertainty assessment [21]. In hydrocarbon reservoir studies, understanding how petrophysical properties vary is vital for exploration and production. Accurate spatial analysis

builds detailed reservoir models by integrating data from well logs, seismic surveys, and core samples [22]. These models identify heterogeneities, fluid flow paths, and estimate reservoir volume. They pinpoint high-permeability and high-porosity areas, guiding optimal well placement [23]. Geoscientists use spatial analysis to assess uncertainty in reservoir characteristics and fluid distribution [24]. This helps engineers decide on field development plans, infill drilling, and waterflood management [25] and [26]. Understanding petrophysical property distribution optimizes production and reduces costs. Monitoring petrophysical property spatial distribution over time using techniques like time-lapse seismic and production logging provides insights into reservoir dynamics and potential changes [27]. This study employs Ordinary Kriging to create petrophysical property surfaces [28]. It's a geostatistical method based on spatial autocorrelation, estimating values at unobserved locations by averaging neighboring data points [29]. Kriging weights are determined by spatial distribution and correlation, minimizing estimation variance [30]. Kriging variance assesses interpolation reliability, aiding decision-making. While OK has many advantages, its reliance on the stationary assumption can lead to inaccuracies in areas with varying spatial correlation [31].

4. Results and Discussion:

1. Petrophysical Properties of the AB Unit: The approach that was previously discussed was used to analyze each well's AB reservoir quantitatively. 45 wells distributed over the study area were used, and these wells were different among them in terms of petrophysical properties. Well Ru-95 was chosen as a key example to represent the study wells, which were logged and assessed using the Techlog program. This choice was based on its distinct characteristic of showing different log readings with depth, effectively highlighting shifts in petrophysical properties. Figure (3) presents an interpretation of the logs related to the petrophysical characteristics of well Ru-95 (for AB1 and AB2). Importantly, the gamma-ray log (GR) registered its highest value at a depth of 3269.4, indicating a significant amount of shale in that region. Similarly, the neutron (NPHI) and density logs (RHOP) also displayed peak values at approximately the same depth, suggesting heightened porosity levels at this specific depth. Moreover, the logs unveiled the presence of hydrocarbons and a notable mixture of sand with varying quantities of shale. This lithological composition primarily results from the reservoir's predominant makeup of sandy formations, interspersed with occasional shale deposits.

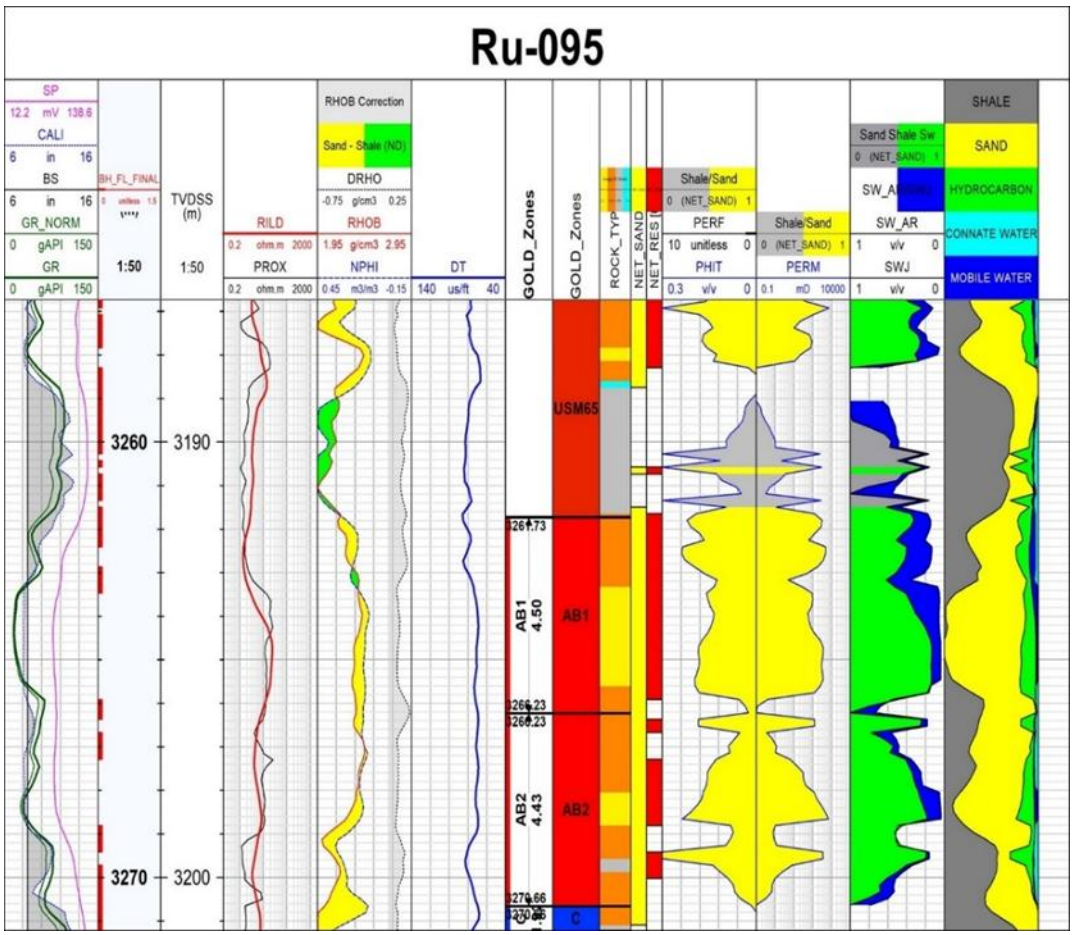

Figure 3: Logs used to infer petrophysical properties of AB unit at RU-95 well

The best of these wells in terms of calculated Petrophysical properties was the RU-01 well. Calculated petrophysical parameters of the RU-01 well are shown in Figures 4(a) and(b). The well has typical values of 0.18 effective porosity, 619.90 md permeability, 93.25% hydrocarbon saturation, and 6.74% water saturation.

Table (1) provides an overview of the findings for the significant petrophysics metrics that are used as variables to assess reservoir quality. The values of these variables are statistically analyzed for each of the designated wells in the research area. Using the porosity formula with shale correction, [32] estimated the reservoirs' porosity from the density log (RHOB) and neutron log (NPHI). The obtained values, which range from 0.06 to 0.20, exhibit outstanding reservoir quality and probably represent well-sorted reservoirs composed of coarse-grained sandstone with low cementation. Since the productivity of a well is associated with the numerical product of thickness (h) and permeability (k) of that unit, the permeability of the reservoir unit is a crucial parameter in the assessment of a well's productivity. The hydrocarbon saturation, Sh, of the hydrocarbon-bearing reservoir units in the research area ranges from 0% to 93.25%, showing that a low percentage of vacant spaces are occupied by water, high hydrocarbon production as well as high hydrocarbon saturation.

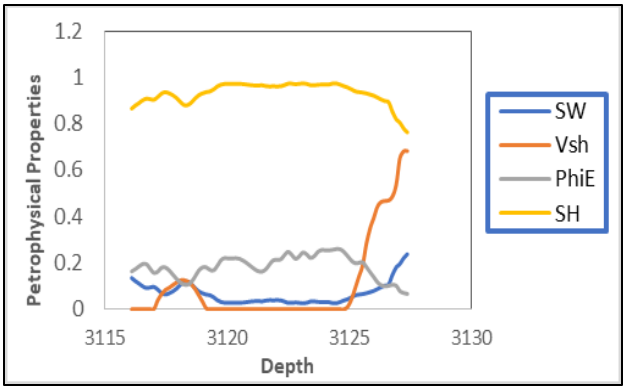

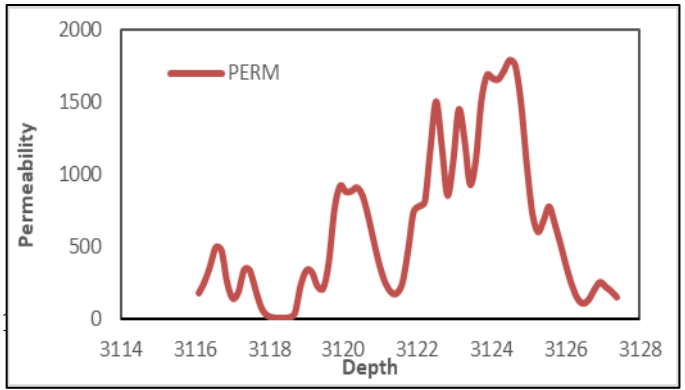

Figure -4 Relationship between (a) effective porosity, water saturation, hydrocarbon saturation, shale volume, and total porosity with depth (b) permeability with depth for RU-01 well.

Table1: Estimated petrophysical properties of the AB unit

No.	Well Name	Top (m)	Bottom (m)	Thickness (m)	Vsh (v/v)	ϕ (v/v)	K (md)	Sw (v/v)	Sh (v/v)
١	Ru-1	3116.1	3127.38	11.28	0.1	0.18	619.9	0.07	0.93
٢	Ru-2	3200.38	3207.24	6.86	0.3	0.11	115.62	-	-
٣	Ru-3	3162.89	3172.49	9.6	0.24	0.14	194.85	0.26	0.74
٤	Ru-4	3101.32	3113.06	11.73	0.3	0.13	-	0.18	0.82
٥	Ru-6	3146.13	3156.95	10.82	0.11	0.16	-	-	-
٦	Ru-7	3135.46	3149.33	13.87	0.07	0.17	624.34	-	-
٧	Ru-20	3208.31	3219.58	11.28	0.19	0.16	454.65	-	-
8	Ru-24	3147.5	3157.25	9.75	0.54	0.03	3.3	0.69	0.31
٩	Ru-26	3148.72	3156.64	7.92	0.23	0.13	259.7	0.34	0.66
١٠	Ru-33	3193.68	3203.28	9.6	0.27	0.1	65.69	0.18	0.82
١١	Ru-36	3362.84	3370	7.16	0.3	0.05	1.69	0.99	0.01
١٢	Ru-40	3133.63	3140.03	6.4	0.42	0.1	241.57	0.28	0.72
١٣	Ru-41	3108.48	3120.07	11.58	0.15	0.17	562.03	0.21	0.79
١٤	Ru-42	3136.53	3140.34	3.81	0.23	0.14	352.55	0.26	0.74
١٥	Ru-43	3161.52	3169.6	8.08	0.37	0.07	14.64	0.47	0.53
١٦	Ru-45	3109.09	3118.54	9.45	0.21	0.13	168.85	0.26	0.74
١٧	Ru-47	3199.01	3211.51	12.5	0.16	0.12	122.04	0.32	0.68
١٨	Ru-48	3151.92	3157.56	5.64	0.57	0.04	10.96	0.65	0.35
١٩	Ru-50	3207.09	3219.74	12.65	0.03	0.16	276.1	0.11	0.89
٢٠	Ru-51	3165.79	3173.25	7.47	0.07	0.17	387.15	0.09	0.91
٢١	Ru-52	3097.82	3109.55	11.74	0.13	0.14	322.07	0.13	0.87
٢٢	Ru-56	3102.54	3106.05	3.51	0.15	0.16	296.74	0.17	0.83
٢٣	Ru-57	3139.12	3147.5	8.38	0.23	0.11	131.94	0.29	0.71
٢٤	Ru-58	3155.42	3162.28	6.86	0.09	0.14	157.96	1	0
٢٥	Ru-95	3263.02	3269.42	6.4	0.21	0.12	135.39	0.36	0.64
٢٦	Ru-97	3163.5	3171.12	7.62	0.16	0.14	158.07	0.23	0.77
٢٧	Ru-98	3298.07	3305.69	7.62	0.2	0.12	117.92	0.28	0.72
٢٨	Ru-100	3236.8	3247.17	10.36	0.13	0.14	148.09	0.24	0.76
٢٩	Ru-101	3226.75	3237.41	10.67	0.12	0.16	335.71	0.21	0.79
٣٠	Ru-103	3307.98	3321.08	13.11	0.07	0.16	262.72	0.48	0.52

٣١	Ru-104	3347.45	3359.03	11.58	0.1	0.17	361.54	0.79	0.21
٣٢	Ru-106	3323.06	3333.27	10.21	0.13	0.13	97.64	0.55	0.45
٣٣	Ru-107	3235.43	3245.95	10.52	0.07	0.15	217.98	0.17	0.83
٣٤	Ru-108	3241.07	3248.08	7.01	0.28	0.09	16.79	0.49	0.51
٣٥	Ru-115	3172.49	3183.46	10.97	0.1	0.16	306.1	0.15	0.85
٣٦	Ru-119	3238.18	3244.12	5.94	0.26	0.1	58.55	0.37	0.63
٣٧	Ru-121	3127.84	3140.18	12.34	0.13	0.17	599.7	0.16	0.84
٣٨	Ru-122	3257.23	3263.17	5.94	0.11	0.13	101.36	0.24	0.76
٣٩	Ru-126	3115.65	3128.14	12.5	0.15	0.15	279.83	0.16	0.84
٤٠	Ru-127	3221.56	3232.84	11.28	0.19	0.15	302.62	0.22	0.78
٤١	Ru-129	3263.32	3271.09	7.77	0.15	0.17	457.62	0.14	0.86
٤٢	Ru-132	3117.48	3128.6	11.13	0.4	0.05	1.58	0.28	0.72
٤٣	Ru-134	3249.45	3263.02	13.56	0.11	0.15	230.68	0.19	0.81
٤٤	Ru-136	3127.84	3138.66	10.82	0.15	0.13	129.25	0.18	0.82
٤٥	Ru-138	3114.43	3121.13	6.7	0.15	0.11	93.45	0.23	0.77

2. Statistical analysis of the petrophysical properties: Before proceeding with any further analysis, it is critical to thoroughly understand the basic statistical features of the petrophysical properties. Understanding the data can aid in the formulation of better research questions and the selection of appropriate methods for analysis. To begin, compute basic summary descriptive statistics such as mean, median, and standard deviation, as well as learn the shape, size, type, and general layout of the data. This can be useful for gaining an understanding of the data's characteristics and identifying potential biases or limitations [18]. Table (2) presents the basic descripting statistical parameters of the petrophysical properties. The findings indicated that the minimum and maximum values of the AB reservoir unit thickness were 3.51 to 13.87 m with an average of 9.37 m indicating this unit is slightly thinner compared with other unit in the main pay zone of Zubair Formation. The mean (9.37) is less than the median (9.75), which suggests that the probability distribution is slightly negatively skewed, which is a true in our case where the skewness coefficient is (-0.31). In other words, the left tail of the distribution might be slightly longer or stretched out compared to the right tail (Figure 4). The standard deviation (2.63) represents the spread of the data points around the mean. With a coefficient of variation (CV) of 28.09%, we can infer that the standard deviation is approximately 28.09% of the mean. This indicates a moderate relative variability compared to the mean. A kurtosis value of (-0.79) suggests that the distribution has negative kurtosis. Negative kurtosis means that the distribution has thinner or lighter tails than a normal distribution, indicating fewer extreme outliers (platykurtic).

The Vsh has a mean value of 0.19, with values ranging from 0.03 to 0.57. The median is 0.15 which indicates that half of the data points are below 0.15 and the other half are above it. The mean and median values are slightly different meaning that the probability distribution of Vsh is not a normal one. The data has a moderate positive skewness, indicating a longer tail on the right side of the distribution (Figure 5), meaning that the data has more outliers on the higher end. Additionally, the Vsh data has a positive kurtosis, indicating that it has heavier tails and more extreme values compared to a normal distribution (leptokurtic). The coefficient of variation is relatively high, suggesting a significant relative variability compared to the mean.

The values range 0.03 – 0.18 with an average of 0.13. The median value is 0.14 and is similar to the mean which may indicates that the probability distribution is normal or close to normal. The standard deviation is small (0.037) which indicates that the data points are relatively close to the mean. The coefficient of the variation is relatively moderate (28.57), indicating a moderate relative variability compared to the mean. The data has a moderate negative skewness, indicating that is somewhat left-skewed. The data of has a kurtosis value slightly greater than 0, suggesting that it has slightly heavier tails than a normal distribution (platykurtic).

From the statistics of k, it can be inferred that the variable has an average value of 227.8, with a range of values from 1.6 to 624.3 (Table 2). The data has a moderate positive skewness, indicating that it is somewhat right-skewed, Figure (5). Additionally, the data has a kurtosis value very close to 0, suggesting that it closely resembles a normal distribution in terms of tailedness and peak (platykurtic). The coefficient of variation is relatively high, indicating a significant relative variability compared to the mean, which suggests that the data points are more dispersed around the mean.

In the case of Sw, the variable has a mean value of 0.31 and a range of values from 0.07 to 1. (Table 2.). The data has a relatively high positive skewness, indicating that it is skewed to the right and has more extreme values on the higher end. Furthermore, the data has a positive kurtosis, indicating that it has heavier tails and a sharper peak than a normal distribution (leptokurtic). The coefficient of variation is relatively high, indicating significant relative variability relative to the mean, implying that the data points are more evenly distributed around the mean.

Table 2 - Statistical analysis of petrophysical properties

Variable	Minimum	Maximum	Mean	Median	StDev	CoefVar	Skewness	Kurtosis
Thickness (m)	3.51	13.87	9.37	9.75	2.634	28.09	-0.31	-0.79
Vsh (v/v)	0.03	0.57	0.19	0.15	0.1193	60.78	1.43	2.13
ϕ(v/v)	0.03	0.18	0.13	0.14	0.0372	28.57	-1.13	0.81
k (md)	1.6	624.3	227.8	194.8	172.4	75.67	0.78	0.01
Sw (v/v)	0.07	1	0.31	0.24	0.2248	70.51	1.74	2.67
Sh (v/v)	0	0.93	0.68	0.76	0.2248	33	-1.74	2.67

Finally, the Sh variable has a mean value of 0.68, with values ranging from 0 to 0.93. The data has a moderate negative skewness, indicating that it is somewhat left-skewed. Additionally, the data has a positive kurtosis, suggesting that it has heavier tails and a sharper peak compared to a normal distribution. The coefficient of variation is relatively moderate, indicating moderate relative variability compared to the mean, which suggests that the data points are somewhat dispersed around the mean.

Overall, the statistical analysis can be summarized by the following points:

1. Most variables have non-normal probability distributions, indicated by differences between mean and median values.

2. Skewness and kurtosis values vary among the variables, suggesting different degrees of asymmetry and tailedness in their distributions.

3. The coefficient of variation (CV) is relatively high for most variables, indicating significant relative variability compared to the mean.

4. Some variables have heavier tails and more extreme values (higher kurtosis), while others have lighter tails (lower kurtosis) compared to a normal distribution.

5. The spread of data points around the mean (standard deviation) varies among variables.

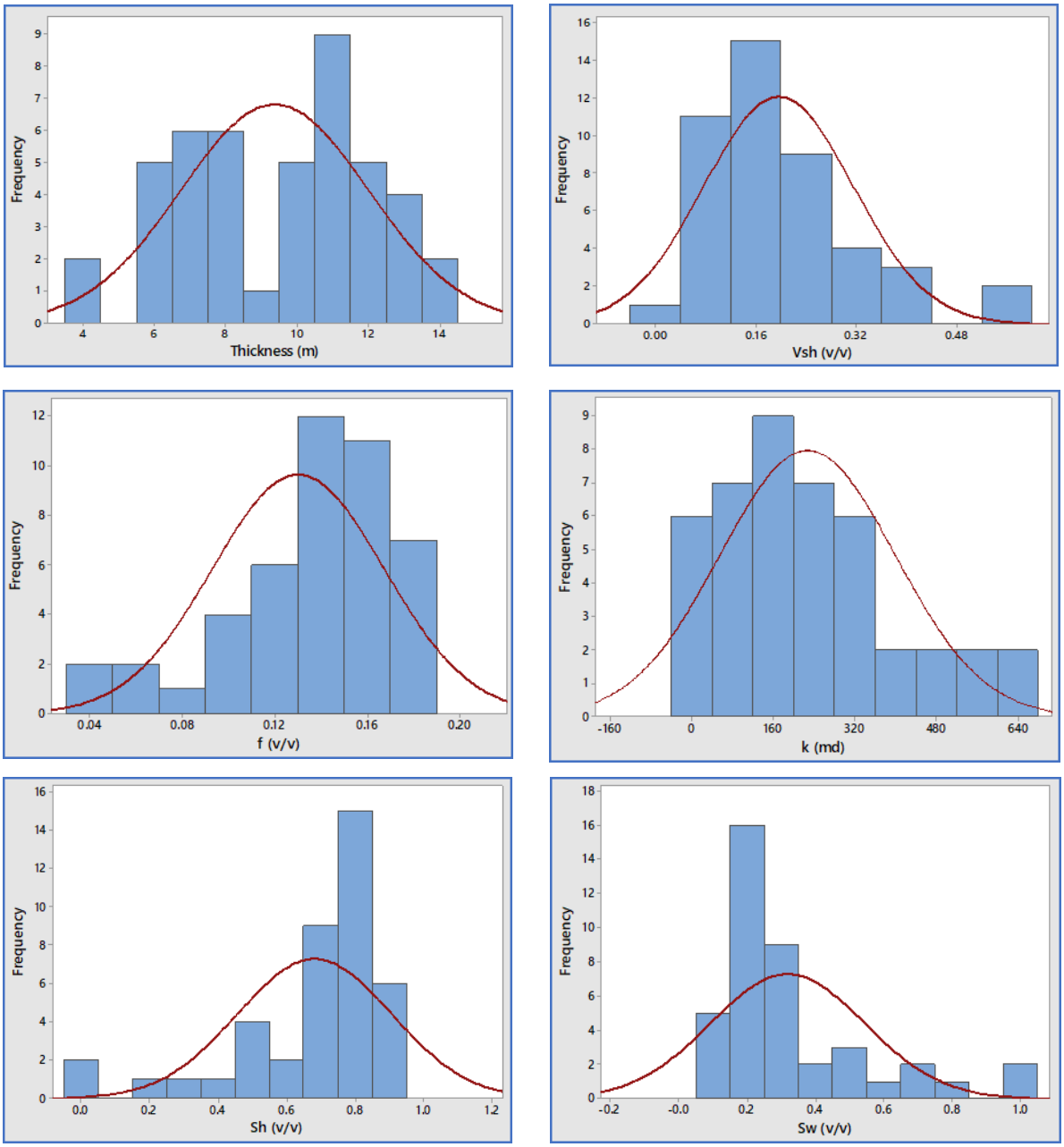

Figure 5: Probability distribution of petrophysical properties

Spatial distribution of the petrophysical properties

By analyzing petrophysical properties spatially, we can identify high-productive areas, estimate hydrocarbon reserves. The ordinary kriging stochastic spatial distribution technique was used to generate the petrophysical property surfaces in this study. It is based on the spatial autocorrelation principle and employs a mathematical framework to estimate unknown values at unobserved locations.

Figures (6 a-d) illustrate that the thickness, porosity, and permeability of the reservoir unit share a consistent pattern of distribution, which is opposite to that of the shale volume. The regions in the northern, middle, and south western parts of the area predominantly exhibit high values for these three characteristics, while the remaining areas display lower values. Conversely, high values of shale volume correspond to lower values of the aforementioned characteristics, and vice versa. It is well-established that shale volume is responsible for reducing the porosity and permeability of rocks, consequently impeding fluid flow within the reservoir unit. Thus, the distribution of petrophysical properties (porosity and permeability) inversely mirrors the distribution of shale volume, which is precisely observed in our study.

The Sw and Sh are not considered in this section, as they are subject to continuous changes due to production and injection rates

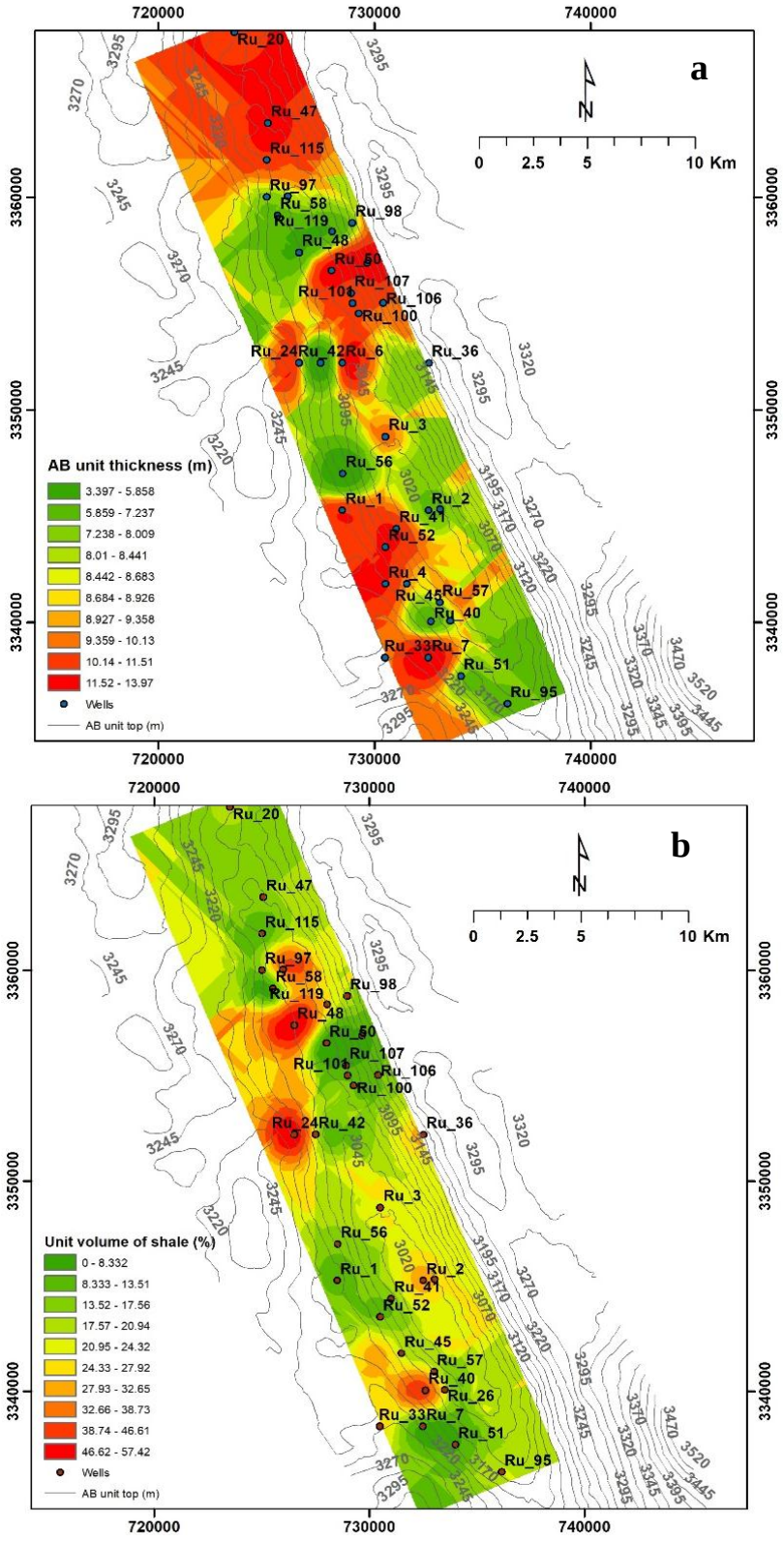

Figure 6: Interpolated surfaces of petrophysical properties (a) unit thickness (m) (b) Vsh (v/v)

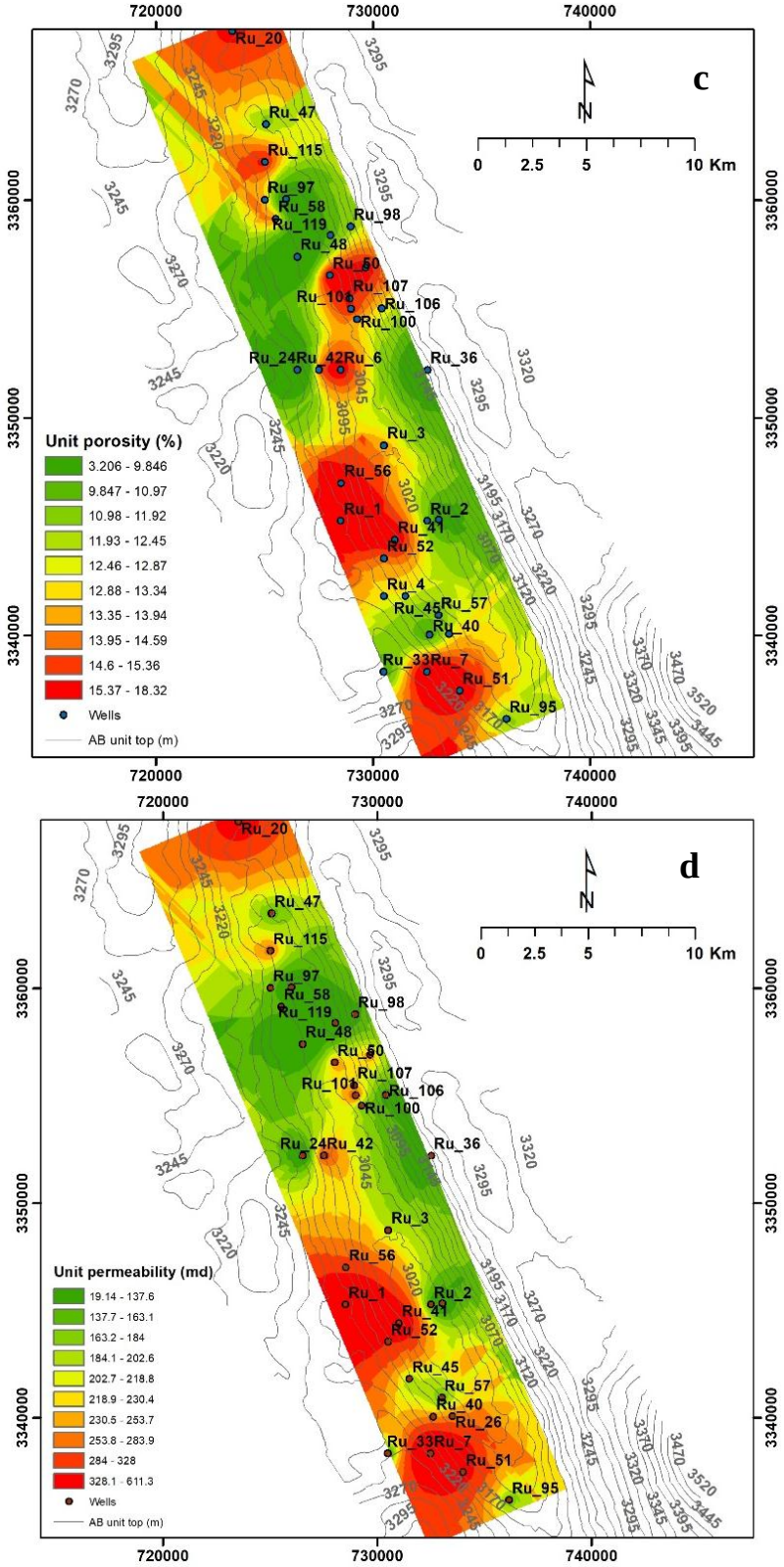

Figure 6: Interpolated surfaces of petrophysical properties (c) porosity (v/v) (d) permeability (md).

6. Conclusion: The Rumaila oilfield's Zubair Formation's lithology is predominantly composed of sandstone with lesser amounts of shale, siltstone, and limestone. The sandstone is the primary reservoir rock for the oil and is characterized by its high porosity and permeability, which allows for the storage and flow of hydrocarbons. In this

study, a comprehensive analysis of the petrophysical properties of the AB unit within the study area was conducted using data from 45 wells.
The logs for well Ru-95 provided insights into the petrophysical characteristics of the AB1 and AB2 layers. The gamma-ray log indicated high shale content at a specific depth, while the neutron and density logs revealed elevated porosity at the same depth, indicating the presence of hydrocarbons in a predominantly sandy reservoir mixed with shale.

Among the wells analysed, RU-01 exhibited favourable petrophysical properties, boasting effective porosity of 0.18, permeability of 619.90 md, hydrocarbon saturation of 93.25%, and water saturation of 6.74%. The statistical analysis highlighted the variability in petrophysical properties, indicating non-normal probability distributions and varying degrees of skewness and kurtosis. The coefficient of variation (CV) suggested significant relative variability compared to the mean, reflecting distinct data spread around the average.

Spatial distribution analysis, crucial for reservoir management and development, employed Ordinary Kriging to generate petrophysical property surfaces. The technique's utilization of spatial autocorrelation enabled interpolation of unknown values based on neighbouring data points. The resulting property surfaces demonstrated consistent patterns, with regions in the northern, middle, and south western parts exhibiting higher values of thickness, porosity, and permeability, while lower values corresponded to higher shale volume. This inverse relationship underscores the influence of shale volume on porosity and permeability.

The study contributes valuable insights for hydrocarbon exploration, field development, and production strategies. The understanding of petrophysical properties and their spatial distribution aids in identifying optimal well placement, assessing reservoir quality, and making informed decisions for reservoir management. While the Ordinary Kriging technique offers robust interpolation and estimation capabilities, its assumption of stationary should be considered, acknowledging potential discrepancies in geographic correlation. As the study omits continuous changes in hydrocarbon and water saturations due to production and injection rates, future work should focus on monitoring these dynamic parameters to further enhance reservoir understanding and management strategies.

References

[1] Macini and Mesini, "Petrophysics and Reservoir Characteristics," pp. 1-20. 2008

[2] Amigun, J. O., & Odole, O. A. “Petrophysical properties evaluation for reservoir characterisation of Seyi oil field (Niger-Delta)”, International Journal of innovation and applied studies, 3(3), 756-773. 2013

[3] Abdolla, E., “Evaluation of Petrophysical Properties of an Oil Field and their effects on production after gas Injection”, In 1st International Applied Geological Congress, Department of Geology, Islamic Azad University–Mashad Branch, Iran (pp. 26-28). 2010

[4] Al-Mudhafar, W. J, “Bayesian kriging for reproducing reservoir heterogeneity in a tidal depositional environment of a sandstone formation”, Journal of Applied Geophysics, 160, 84-102. 2019

[5] Shaker, N., Al-Mayyahi, H. K., & Al-Malikee, H. S., “Variation of saturation pressure values in Mishrif and Zubair ReservoirS in Rumaila Oilfield, Southern Iraq”, The Iraqi Geological Journal, 16-31. 2020

[6] Al-Sakini, J. A., “Summary of petroleum geology of Iraq and the Middle East”, Northern Oil Company Press (Naft-Al Shamal Co.) Kirkuk, Iraq (in Arabic). 1992

[7] Aqrawi, A. A., Goff, J. C., Horbury, A. D., & Sadooni, F. N., “The petroleum geology of Iraq”, Scientific press. 2010

[8] Van Bellen, R.C., H.V. Dunnington, and R. Wetzel, Lexique Stratigraphique International center,

National de La Recherche Scientique III, Asie, Fascicule 10a, Paris, 333 p. 1959

[9] Worthington, P. F., "The evolution of shaly-sand concepts in reservoir evaluation", The Log Analyst, 26(01). 1985

[10] Larionov, V. V., "Radiometry of boreholes", Nedra, Moscow, 127. 1969

[11] Asquith, G. B., Krygowski, D., & Gibson, C. R., "Basic well log analysis", (Vol. 16). Tulsa: American Association of Petroleum Geologists. 2004

[12] Schlumberger, "Log Interpretation Principles/Applications", 3rd ed. 1991

[13] Dresser Atlas, "Log Interpretation Charts", Dresser Industries Inc., Houston, Texas. 107p. 1979

[14] Tiab, D., & Donaldson, E. C. "Petrophysics: theory and practice of measuring reservoir rock and fluid transport properties", Gulf professional publishing. 2015

[15] Abdulmajeed, Y. N., Ramadhan, A. A., & Mahmood, A. J., "Comparing between permeability prediction by using classical and FZI methods/Tertiary Reservoir in Khabaz Oil Field/Northern Iraq", Iraqi Journal of Oil and Gas Research (IJOGR), 2(1), 45-54. 2022

[16] Amaefule, J. O., Altunbay, M., Tiab, D., Kersey, D. G., & Keelan, D. K., 'Enhanced reservoir description: using core and log data to identify hydraulic (flow) units and predict permeability in uncored intervals/wells", In SPE annual technical conference and exhibition. OnePetro, 1993, October.

[17] Balan, B., Mohaghegh, S., & Ameri, S., "State-of-the-art in permeability determination from well log data: Part 1-A comparative study, model development", In SPE Eastern Regional Meeting (pp. SPE-30978). SPE. 1995, September

[18] Schlumberger, "Petrel online help, Petrel Introduction Course Schlumberger ", pp. (560). 2009

[19] Schlumberger, "Log interpretation principles/applications", Schlumberger Company Publication, Houston, Texas, pp 3–10. 1987

[20] Archie, G. E., (1942), "The electrical resistivity log as an aid in determining some reservoir characteristics", Transactions of the AIME, 146(01), 54-62.

[21] BOSTAN, P., "Basic kriging methods in geostatistics", Yuzuncu Yıl University Journal of Agricultural Sciences, 27(1), 10-20. 2017

[22] Moore, W. R., Ma, Y. Z., Pirie, I., & Zhang, Y., "Tight gas sandstone reservoirs, part 2: Petrophysical analysis and reservoir modeling", In Unconventional Oil and Gas Resources Handbook (pp. 429-448). Gulf Professional Publishing. 2016

[23] Handhal, A. M., Hussein, A. A., Al-Abadi, A. M., & Ettensohn, F. R., "Spatial Modeling of Hydrocarbon Productivity in the Nahr Umr Formation at the Luhais Oil Field, Southern Iraq", Natural Resources Research, 30, 765-787. 2021

[24] Ebong, E. D., Akpan, A. E., & Ekwok, S. E., "Stochastic modelling of spatial variability of petrophysical properties in parts of the Niger Delta Basin, southern Nigeria", Journal of Petroleum Exploration and Production Technology, 10, 569-585. 2020

[25] Moolya, A., Rodríguez-Martínez, A., & Grossmann, I. E., "Optimal producer well placement and multiperiod production scheduling using surrogate modeling", Computers & Chemical Engineering, 165, 107941. 2022

[26] Simonov, M., Shubin, A., Penigin, A., Perets, D., Belonogov, E., & Margarit, A., "Optimization of oil field development using a surrogate model: case of miscible gas injection", In SPE Reservoir Characterisation and Simulation Conference and Exhibition. OnePetro. 2019, September

[27] Djuraev, U., Jufar, S. R., & Vasant, P., "A review on conceptual and practical oil and gas reservoir monitoring methods", Journal of Petroleum Science and Engineering, 152, 586-601. 2017

[28] Wackernagel, H., "Multivariate geostatistics: an introduction with applications", Springer Science & Business Media. 2003

[29] Cressie, N., "Spatial prediction and ordinary kriging", Mathematical geology, 20, 405-421. 1988

[30] Dimitrakopoulos, R., & Luo, X., "Spatiotemporal modelling: covariances and ordinary kriging systems", In Geostatistics for the Next Century: An International Forum in Honour of Michel David's Contribution to Geostatistics, Montreal, 1993 (pp. 88-93). Dordrecht: Springer Netherlands. 1994

[31] Berman, J. D., Breysse, P. N., White, R. H., Waugh, D. W., & Curriero, F. C., "Evaluating methods for spatial mapping: Applications for estimating ozone concentrations across the contiguous United States", Environmental Technology & Innovation, 3, 1-10. 2015

[32] Cannon, S., "Petrophysics: a practical guide", John Wiley & Sons. 2015